A new approach towards ferromagnetic conducting materials based on TTF-containing polynuclear complexes

Sergey V. Kolotilov, Olivier Cador, Fabrice Pointillart, Stéphane Golhen, Yann Le Gal, Konstantin S. Gavrilenko, Lahcène Ouahab

A new approach towards ferromagnetic conducting materials based on TTF-containing polynuclear complexes†‡

Sergey V. Kolotilov,[ab] Olivier Cador,[b] Fabrice Pointillart,[b] Stéphane Golhen,[b] Yann Le Gal,[b] Konstantin S. Gavrilenko[a] and Lahcène Ouahab*[b]

Received 1st December 2009, Accepted 24th March 2010
DOI: 10.1039/b925178b

Five complexes containing binuclear cation $[Cu_2(LH)_2]^{2+}$ (LH_2 = 1 : 2 Schiff base of 1,3-diaminobenzene and butanedione monoxime) were prepared and characterized. Metathesis of one perchlorate anion in $[Cu_2(LH)_2(H_2O)_2](ClO_4)_2$ (**1**) by anionic TTF-carboxylate (TTF–CO_2^-) leads to the complex $[Cu_2(LH)_2(CH_3OH)_2](TTF–CO_2)(ClO_4)\cdot H_2O$ (**2**). Reactions of **1** with substituted pyridines bipy, dpe and TTF–CH = CH–py result in formation of the complexes $\{[Cu_2(LH)_2(bipy)](ClO_4)_2\}_n\cdot 2nH_2O$ (**3**), $[Cu_2(LH)_2(dpe)_2](ClO_4)_2\cdot 2CH_3OH$ (**4**) and $[Cu_2(LH)_2(TTF–CH = CH–py)(H_2O)](ClO_4)_2\cdot 1.5H_2O$ (**5**), where bipy = 4,4′-bipyridine, dpe = *trans*-(4-pyridyl)-1,2-ethylene and TTF–CH = CH–py = 1-(2-tetrathiafulvalenyl)-2-(4-pyridyl)ethylene. Whereas complex **2** is built from discrete ionic particles (with rather long Cu–S contacts), compounds **1** and **3** contain 1D polymeric chains, in which structural units are bonded through Cu–O bonds or through bridging bipy molecule, respectively. Dinuclear complexes **4** and **5** are linked though π-stacking of dpe or TTF–CH = CH–py, respectively. All complexes are characterized by dominating ferromagnetic behavior with J values in the range from +9.92(8) cm^{-1} to +13.4(2) cm^{-1} for Hamiltonian $H = -JS_1S_2$. Magnetic properties of the compounds, containing stacks of aromatic molecules in crystal structures (**4** and **5**), correspond to ferromagnetic intradimer and antiferromagnetic intermolecular interactions ($zJ' = -0.158(3)$ and $-0.290(2)$ cm^{-1}, respectively). It was found that TTF–CH = CH–py ligand in $[Cu_2(LH)_2(TTF–CH = CH–py)(H_2O)]^{2+}$ could be electrochemically oxidized to cation-radical form in the solution.

Introduction

Compounds possessing at least two different properties, which may find practical applications, are considered as promising candidates for creation of multifunctional materials, in particular, conducting magnetic materials.[1] Such properties may originate from the presence of different structural elements in the compound, for example, different "building blocks" responsible for ferromagnetism and conductivity.[2] This approach to conducting magnetic materials is based on combination of a "conducting component" (for example, oxidised tetrathiafulvalene, which bears unpaired electrons on π-orbitals) and a 3d metal, with unpaired electrons on the d-orbitals. Several mono- and polynuclear complexes with TTF-containing ligands were reported recently,[3] however the reported polynuclear complexes, containing TTF, are characterized by antiferromagnetic exchange.[3b,c] Here we present the strategy, which allowed us to prepare two TTF-containing binuclear complexes with ferromagnetic exchange interactions between Cu^{II} ions. One of these compounds contains anionic 2-tetrathiafulvalenylcarboxylate (hereinafter referred to as TTF–CO_2^-) as a counterion in the lattice, while the second contains covalently bridged 1-(2-tetrathiafulvalenyl)-2-(4-pyridyl)ethylene (TTF–CH = CH–py). These complexes, containing ferromagnetically-coupled polynuclear blocks and TTF derivatives, can be considered as the precursors for multifunctional materials.

A copper(II) complex with Schiff base, derived from 1,3-diaminobenzene and monoxime of butanedione (hereinafter referred to as LH_2, Fig. 1) of composition $[Cu_2(LH)_2(H_2O)_2](ClO_4)_2$ (compound **1**) was taken as the starting material due to several reasons. First, Cu^{II} ions are linked through the 1,3-phenylene bridge, which normally mediates ferromagnetic interactions between paramagnetic centers.[4] Second, Cu^{II} ions can coordinate additional ligands, which allows one to consider this molecule as suitable building block for creation of more complex structures. The derivatives of TTF were chosen as the component, which potentially may give rise to conductivity.

We used two ways to introduce the TTF-containing molecule as a potential conductive component: (i) anionic TTF–CO_2^-, which replaced one of perchlorate anions and counter-balanced positive charge of a dicopper cation, and (ii) neutral TTF–CH=CH–py, which was covalently linked to a dicopper unit due to coordination of pyridine unit to Cu^{II}.

[a]*L. V. Pisarzhevskii Institute of Physical Chemistry of the National Academy of Sciences of the Ukraine, Prospekt Nauki 31, Kiev, 03028, Ukraine*

[b]*Equipe Organométalliques et Matériaux Moléculaires, Sciences Chimiques de Rennes, UMR UR1-CNRS 6226, Université de Rennes 1, Campus de Beaulieu, 35042 Rennes cedex, France. E-mail: lahcene.ouahab@univ-rennes1.fr; Fax: +33 (0)2 23 23 68 40; Tel: +33 (0)2 23 23 56 59*

† This paper is part of a *Journal of Materials Chemistry* themed issue on Advanced Hybrid Materials, inspired by the symposium on Advanced Hybrid Materials: Stakes and Concepts, E-MRS 2010 meeting in Strasbourg. Guest editors: Pierre Rabu and Andreas Taubert.

‡ CCDC reference numbers 756226–756230. For crystallographic data in CIF or other electronic format see DOI: 10.1039/b925178b

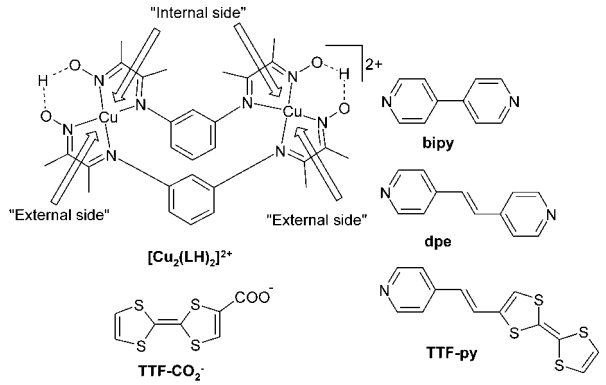

Fig. 1 Drawings of V-shape cation $[Cu_2(LH)_2]^{2+}$ and ligands, used in this study, along with their abbreviations. Arrows indicate positions in the coordination spheres of Cu^{II} ions which may be occupied by donor atoms.

Metathesis of one perchlorate ion in $[Cu_2(LH)_2(H_2O)_2](ClO_4)_2$ by one $TTF–CO_2^-$, associated with H_2O substitution by CH_3OH, gave compound **2**, $[Cu_2(LH)_2(CH_3OH)_2](TTF–CO_2)(ClO_4)\cdot H_2O$. Several complexes with similar pyridine-containing molecules (bipy, dpe and TTF–CH=CH–py, Fig. 1) were prepared in order to see the influence of ligand structure on the composition, crystal packing and magnetic properties of coordination compounds. All these three ligands contain pyridine rings, linked with an additional substituent:

- pyridine ring, attached through single C–C bond, where both these C atoms belong to pyridine cycles, that is 4,4′-bipyridine (bipy);
- pyridine ring, attached through bridging –CH=CH– group, that is *trans*-(4-pyridyl)-1,2-ethylene (dpe);
- TTF fragment, attached through bridging –CH=CH– group (TTF–CH=CH–py).

This row of ligands allowed us to see the influence of the "additional component", linked to coordinated pyridine ring (such as –py, –CH=CH–py and –CH=CH–TTF), on the structures and magnetic properties of coordination compounds based on the $Cu_2(LH)_2^{2+}$ building block.

Reaction of the starting compound **1** with bipy gave a 1 : 1 adduct possessing a 1D chain structure (compound **3**, $\{[Cu_2(LH)_2(bipy)](ClO_4)_2\}_n\cdot 2nH_2O$), whereas reaction of **1** with dpe produced 1 : 2 adduct (compound **4**, $[Cu_2(LH)_2(dpe)_2](ClO_4)_2\cdot 2CH_3OH$). Finally, reaction of **1** with TTF–CH=CH–py resulted in formation of a 1 : 1 adduct (compound **5**, $Cu_2(LH)_2(TTF–CH=CH–py)(H_2O)(ClO_4)_2\cdot 1.5H_2O$).

Results and discussion

Synthesis

Starting compound $[Cu_2(LH)_2(H_2O)_2](ClO_4)_2$ was prepared by *in situ* formation of a Schiff base of 1,3-diaminobenzene and monoxime of butanedione (Fig. 1). No isolation of the ligand was required, similarly to Schiff base formation from 4,4′-diphenyldiamine and the same ketone in the presence of Cu^{II} salts[5] and in contrast to the procedure reported for synthesis of similar compounds, where intermediate isolation of the ligand was performed.[6]

The binuclear cation of **1** may be represented as two "CuN" parts, linked by 1,3-phenylene units, which give V-shape particles (as it was confirmed by X-ray structure determination, *vide infra*). It potentially contains four vacant positions in coordination spheres of Cu^{II} ions, two on "external" and two on "internal" sides of the V-shape particles, and all these positions are available for the coordination of donor molecules.

Crystallization of $Cu_2(LH)_2^{2+}$ with $TTF–CO_2^-$ from methanol produced $Cu_2(LH)_2(CH_3OH)_2(TTF–CO_2)(ClO_4)\cdot H_2O$ (compound **2**) regardless of the ratio between $Cu_2(LH)_2^{2+}$ and $(TTF–CO_2)^-$ in the reaction mixture (1 : 1 or 1 : 2). It seems that the main driving force for precipitation of **2** is the solubility of this compound, which is probably lower than the solubility of both corresponding salts of cation of **1** with two perchlorates or two TTF-carboxylates as counter-ions.

Two CH_3OH molecules are coordinated to two Cu^{II} ions in **2** (*vide infra*), however recrystallization of this compound from nitromethane (performed in attempt to induce dissociation with decoordination of CH_3OH and coordination of $TTF–CO_2^-$ to Cu^{II}) gave the same complex **2** as the only crystalline product. It may be concluded that the stability constant of the methanol adduct (in respect of dissociation to $Cu_2(LH)_2^{2+}$ and CH_3OH) is high, or again, the solubility of compound **2** is much lower compared to the solubilities of possible complexes, which do not contain coordinated methanol molecules.

Interactions of discrete binuclear particles $Cu_2(LH)_2^{2+}$ in solution with corresponding substituted pyridines lead to the formation of **2–5**. In particular, the reaction with an excess of bipy resulted in the precipitation of a 1 : 1 adduct (**3**), reaction with an excess of dpe led to a 1 : 2 adduct (**4**), and reaction with TTF–CH=CH–py again results in the formation of a 1 : 1 adduct (**5**) even in an excess of the ligand. As in the case of the above compound **2**, crystallization of different products (with different Cu_2–pyridine ratios, 1 : 1 in **3** and **5** and 1 : 2 in **4**) may be caused by their different solubilities, which are probably governed by the energies of their crystal lattices.

Crystal structures

All compounds **1–5** contain the fragment $[Cu_2(LH)_2]^{2+}$ (Fig. 1) as cationic building block (with different ligands, additionally coordinated to Cu^{II} centers). The structure of this cation is almost the same in all complexes **1–5** as the core of $[Cu_2(LH)_2(H_2O)(ClO_4)]^+$ unit in the structure of compound **1**, and it is described in detail only for this complex.

Compound 1. This compound possesses the structure of a 1D coordination polymer, consisting of binuclear V-shape "building blocks" $[Cu_2(LH)_2(H_2O)_2(ClO_4)]^+$ (Fig. 2). In each such cation two Cu^{II} ions are linked by two anionic fragments HL^- (monodeprotonated ligand LH_2), coordinated *via* imine and oxime nitrogen atoms forming 5-membered metallocycles. A Cu(1) ion is located in a distorted octahedral donor set N_4O_2, nitrogen atoms lie in plane (average Cu(1)–N bonds are 1.99 Å; exact values along with standard deviations are hereinafter presented in Table 1), and axial positions are occupied by oxygen donor atoms: O-atom of coordinated ClO_4^- ion and O-atom of deprotonated oximato group of neighboring binuclear fragment $[Cu_2(LH)_2(H_2O)_2(ClO_4)]^+$ (average Cu(1)–O bonds are 2.61 Å).

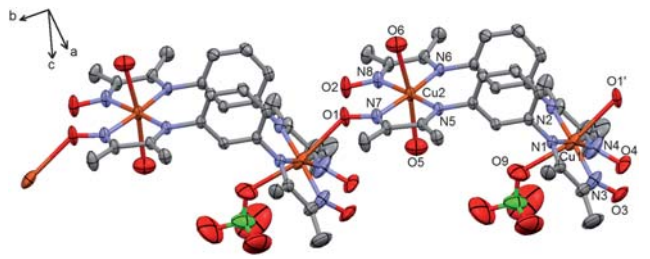

Fig. 2 ORTEP view of the fragment of 1D chain of $[Cu_2(LH)_2(H_2O)_2](ClO_4)_2$ (**1**). Thermal ellipsoids are drawn at 30% probability. Non-coordinated ClO_4^- ions, hydrogen atoms, disordered oxygen atoms and disordered methyl group and are omitted for clarity.

Table 1 Selected bond lengths and distances for **1**

Bond	Length, Å	Bond	Length, Å
Cu(1)–N(1)	2.014(4)	Cu(2)–N(5)	2.022(3)
Cu(1)–N(2)	2.008(4)	Cu(2)–N(6)	2.027(3)
Cu(1)–N(3)	1.978(6)	Cu(2)–N(7)	1.990(3)
Cu(1)–N(4)	1.965(5)	Cu(2)–N(8)	1.974(4)
Cu(1)–O(1)′	2.584(5)	Cu(2)–O(5)	2.500(5)
Cu(1)–O(9)	2.642(5)	Cu(2)–O(6)	2.464(5)

A Cu(2) ion is also located in distorted octahedral environment N_4O_2, where axial positions are occupied by oxygen atoms of coordinated water molecules (Fig. 2). Average Cu(2)–N bonds are almost the same as average Cu(1)–N (2.00 Å). However, Cu(2)–O bonds (2.48 Å in average) are shorter than Cu(1)–O bonds, which may be caused by some steric hindrances in the case of bonds with Cu(1) (since O(1)′ belongs to large binuclear cation, compared to oxygen atoms of water molecules in the case of Cu(2)). The bonds of Cu^{II} and donor atoms in axial positions are longer than the bonds with donors in the equatorial position, evidence for Jahn–Teller distortion.

Cu^{II} ions lie almost exactly in the planes, formed by corresponding coordinated nitrogen donor atoms (N(1),N(2),N(3),N(4) and N(5),N(6),N(7),N(8) for Cu(1) and Cu(2), respectively). The angle between the mean planes N_4 formed by the above mentioned nitrogen atoms, coordinated to Cu(1) and Cu(2), respectively, is 57.14(12)°, which is very close to the expected idealized angle between C–N bonds in 1,3-diaminobenzene (60°). Aromatic rings of two LH^- residues are almost parallel (the angle between mean planes of these rings is 6.38(15)°) and are located at the distance about 3.3 Å from each other.

There are H-atoms between oxygen atoms of oximato-groups O(1), O(2) and O(3), O(4). These H-atoms are involved in H-bonds, which join two dioximate ligands L^{2-} into a pseudo-macrocycle $(LH)_2$, which is typical for complexes of 3d metals with dioximes.[5,7]

As it was mentioned, formation of 1D chains in the crystal of **1** is caused by coordination of deprotonated oxygen atom O(1) of oximato-group of dinuclear unit $[Cu_2(LH)_2(H_2O)_2(ClO_4)]^+$ to Cu(1) ion of neighboring block (Cu(1)–O(1)′ bond length is 2.584(5) Å). These chains are located along the *b* axis. Positive charges of the chains are compensated by non-coordinated ClO_4^- ions, located between them. The distance between Cu ions within a "building block" $[Cu_2(LH)_2(H_2O)_2(ClO_4)]^+$ is 6.9916(9) Å, and the shortest distance between Cu ions of neighboring units through Cu(1)–O(1)′ bond is 5.2407(9) Å.

Compound 2. Compound **2** crystallizes as one cation $[Cu_2(LH)_2(CH_3OH)_2]^{2+}$ with one anion TTF–CO_2^- and one anion ClO_4^- and a solvent H_2O molecule (Fig. 3). This compound contains a dinuclear $Cu_2(LH)_2^{2+}$ cation as the component, responsible for ferromagnetic properties (*vide infra*) and TTF–CO_2^- as the component, which is necessary for conductivity. Coordination polyhedra of both Cu^{II} ions can be considered as highly distorted octahedra CuN_4OD (or square pyramids CuN_4O with additional donor D under the basement), where D is O(4) atom of the neighboring binuclear cation $[Cu_2(LH)_2(CH_3OH)_2]^{2+}$ in the case of Cu(1), and D is S(2) of TTF–CO_2^- in the case of Cu(2). Basal positions of these octahedra are occupied by N-donors of LH^- (Cu–N bonds are 2.00 Å in average). Two coordinated CH_3OH molecules (Cu–O bonds are 2.25 Å in average, Table 2) are located inside V-shape molecule.

There is a tendency towards formation of pseudo-1D chain in compound **2** *via* semi-coordination of O(4) atom of oximato-group to Cu(1) ion of neighboring cation $Cu_2(LH)_2^{2+}$ (Cu(1)–O(4)′ distance is 3.106(8) Å). Cu–Cu distance within binuclear block is 6.779(2) Å, and the shortest Cu–Cu intermolecular contact is 5.833(2) Å (through Cu(1)–O(4)′ contact).

TTF-carboxylate ions are located between these pseudo-1D chains, the shortest contact between metal and TTF-CO_2^- is Cu(2)–S(2) (3.427(3) Å). In contrast, no short contacts between

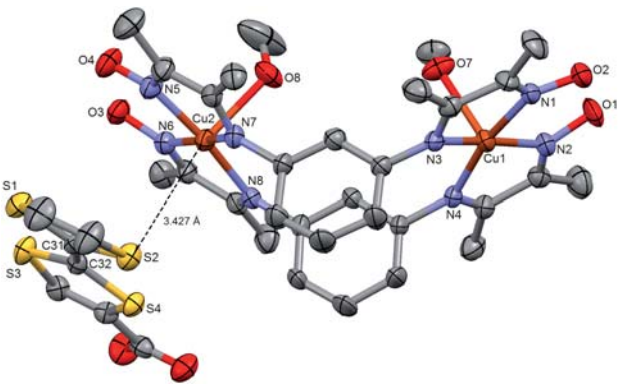

Fig. 3 ORTEP view of the complex $[Cu_2(LH)_2(CH_3OH)_2](TTF–CO_2)(ClO_4)\cdot H_2O$ (**2**) highlighting the Cu(2)–S(2) short contact. Thermal ellipsoids are drawn at 30% probability. Hydrogen atoms, perchlorate anion and non-coordinated water molecule are omitted for clarity.

Table 2 Selected bond lengths and distances for **2**

Bond	Length, Å	Bond	Length, Å
Cu(1)–N(1)	1.974(8)	Cu(2)–N(6)	1.958(8)
Cu(1)–N(2)	1.986(9)	Cu(2)–N(7)	2.007(8)
Cu(1)–N(3)	2.044(9)	Cu(2)–N(8)	2.034(8)
Cu(1)–N(4)	2.029(7)	Cu(2)–O(8)	2.278(8)
Cu(1)–O(7)	2.217(7)	Cu(2)–S(2)	3.427(6)
Cu(1)–O(4)′	3.106(6)	S(2)–S(4)′	3.548(7)
Cu(2)–N(5)	1.975(8)		

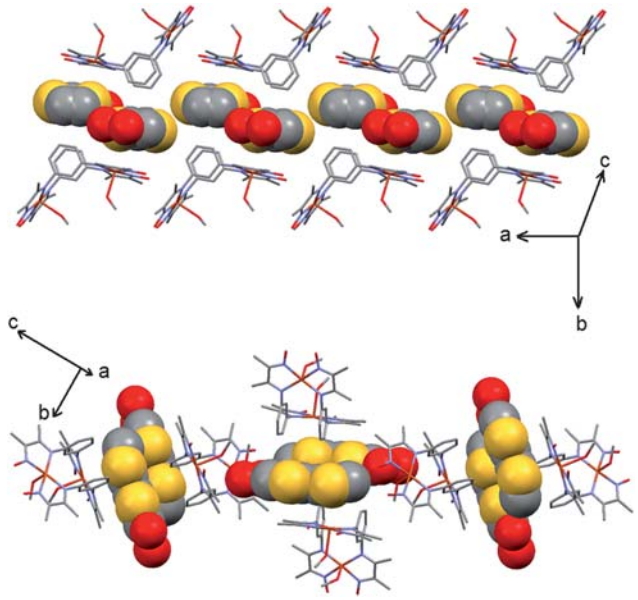

Fig. 4 Crystal packing of **2** highlighting the formation of 1D organic (space fill) and inorganic (capped sticks) networks (up). The bottom figure shows the orientation of the 1D organic networks.

negatively charged oxygen of carboxylic group are observed, which may be caused by more "soft" character of S compared to O^-. The distances between S-atoms of neighbouring TTF–CO_2^- anions are 3.548(4) and 4.066(4) Å, which is close to the sum of the radii of S atoms (about 3.7 Å). From the standpoint of conducting materials development, TTF–CO_2^- ions may be considered as "purely organic" component, located between "metal-containing" pseudo-1D chains (Fig. 4).

The central C–C bond length between two heterocyclic rings of TTF–CO_2^- (C(31)–C(32)) is 1.335(13) Å, which is close to similar bonds in non-oxidized TTF.[8]

Non-coordinated perchlorate anions in **2** are disordered in 2 positions.

Compound 3. $[Cu_2(LH)_2(bipy)]^{2+}$ forms 1D chains, positive charges of Cu^{II} ions are counterbalanced by two ClO_4^- ions per Cu^{II} and the crystal contains three solvated water molecules per Cu_2 unit. One of these H_2O molecules is disordered in two positions with occupation factors 0.7 and 0.3. bipy acts as a bridge between $Cu_2(LH)_2^{2+}$ fragments (Fig. 5). Cu^{II} ions have non-identical donor sets N_5: in coordination spheres of both Cu^{II} ions four nitrogen atoms belong to imine group and oximato groups, and the fifth nitrogen atom of bipy molecule is in axial position, but coordination modes of pyridine rings are different for Cu(1) and Cu(2), *vide infra*. Trigonal distortion index[9] τ is 0.13 for Cu(1) and 0.10 for Cu(2), evidencing that coordination environments of Cu^{II} ions are close to square pyramids. Cu–N bonds with axial nitrogen atoms are longer (Cu(1)–N(9) 2.212(4) Å and Cu(2)–N(10) (2.279(4) Å) than Cu–N bonds with N donors in plane (2.01 in average, Table 3). The mode of coordination of bipy to Cu(1) through N(9) atom is quite expected,[5b] whereas coordination of bipy to Cu(2) through N(10) atom is not typical, since bipy molecule is "inclined" towards CuN_4 plane: the angle between mean plane N_4 (a plane in coordination environment of Cu(2)) and mean plane of pyridine ring,

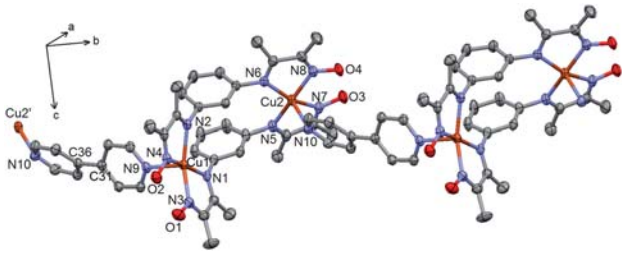

Fig. 5 ORTEP view of the 1D complex $\{[Cu_2(LH)_2(bipy)](ClO_4)_2\}_n \cdot 2nH_2O$ (**3**). Thermal ellipsoids are drawn at 30% probability. Hydrogen atoms, ClO_4^- anions and solvent water molecules are omitted for clarity.

coordinated to Cu(2), is 47.44(13)°, whereas the angle between the mean plane N_4 (a plane in coordination environment of Cu(1)) and the mean plane of pyridine ring, coordinated to Cu(1), is 83.93(11)°. "Typical" coordination of pyridine ring to Cu^{II} occurs on the "external side" of a V-shape dicopper block, whereas "non-typical" coordination takes place on the "internal side" of a V-shape molecule.

The angle between aromatic rings of bipy molecule is 32.36(15)°. The distance of Cu(1)–Cu(2) within $[Cu_2(LH)_2]^{2+}$ is 7.0352(8) Å, and the separation between Cu(1) and Cu(2)′ through the bipy bridge is 11.0440(8) Å. The C(31)–C(36) bond between aromatic rings of bipy is 1.496(6) Å, which is close to the expected value for a single bond and is evidence for the absence of conjugation between the pyridine rings. 1D chains, formed by $[Cu_2(LH)_2(bipy)]^{2+}$, are located in one layer parallel to the *ab* plane, and counterions (ClO_4^-) fill the space between such layers. The O(3) oxygen atom of the oxime group is located at 3.328(4) Å from the Cu(1)′ ion of the neighboring molecule. Though the Cu^{II} and oxygen at such distance can not be considered to be bonded, this observation is in line with the tendency to form pseudo-1D chains, previously found in the case of **1** and **2**. The distance Cu(1)–Cu(2)′ (through Cu(1)–O(3)′ contact) is 6.0552(7) Å, which is the shortest Cu–Cu contact in this compound.

Compound 4. This compound crystallizes as discrete cations $[Cu_2(LH)_2(dpe)_2]^{2+}$ with two ClO_4^- anions and two methanol molecules per dicopper cation. The cation $[Cu_2(LH)_2(dpe)_2]^{2+}$ has a symmetry plane. Both Cu^{II} ions are located in identical square-pyramidal donor sets N_5 (τ = 0.095),[9] containing four N-atoms of imine and oximato- groups in the base of square pyramid (average Cu–N bond is 2.02 Å) and N atom from aromatic heterocycle of dpe in axial position (Cu–N_{py} 2.223(4) Å). Each dpe molecule is coordinated to a Cu^{II} ion in a monodentate mode (through only one nitrogen atom) from the "external side" of a V-shape dicopper block, and the second nitrogen donor is not coordinated (Fig. 6). Two methanol

Table 3 Selected bond lengths and distances for **3**

Bond	Length, Å	Bond	Length, Å
Cu(1)–N(4)	1.981(4)	Cu(2)–N(7)	1.992(4)
Cu(1)–N(3)	1.988(4)	Cu(2)–N(8)	1.988(4)
Cu(1)–N(1)	2.033(4)	Cu(2)–N(5)	2.026(4)
Cu(1)–N(2)	2.051(4)	Cu(2)–N(6)	2.033(4)
Cu(1)–N(9)	2.212(4)	Cu(2)–N(10)	2.279(4)

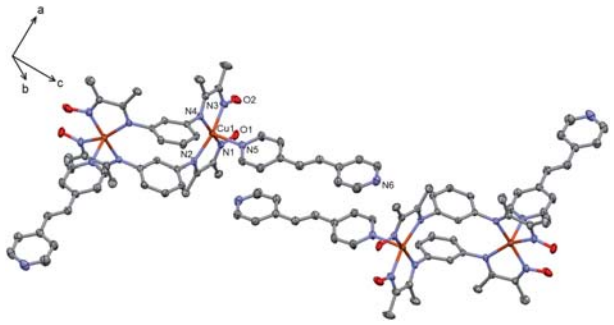

Fig. 6 ORTEP view of the complex $[Cu_2(LH)_2(dpe)_2](ClO_4)_2 \cdot 2CH_3OH$ (**4**). Thermal ellipsoids are drawn at 30% probability. Hydrogen atoms, perchlorate anion and methanol molecule are omitted for clarity.

molecules are located nearby Cu^{II} ions (distance Cu–O is 3.117(15) Å, Table 4).

In the crystal each dpe molecule of $[Cu_2(LH)_2(dpe)_2]^{2+}$ cation lies over another dpe molecule of the neighboring $[Cu_2(LH)_2(dpe)_2]^{2+}$ cation. The planes of adjacent dpe molecules are exactly parallel and the distance between their mean planes is 3.598(5) Å. Such arrangement of dpe may be the indication of π–π interactions between these molecules (Fig. 6). Thus, neighboring $[Cu_2(LH)_2(dpe)_2]^{2+}$ cations form 1D chains (located parallel to *a*+*c* diagonal of the unit cell); binuclear units in such chain are hold by stacking interactions.

The Cu(1)–Cu(1)′ distance within one binuclear fragment $Cu_2(LH)_2^{2+}$ is 7.1433(6) Å, which is the shortest Cu–Cu separation in **4**. The shortest Cu–Cu *intermolecular* contact is 9.0890(6) Å, whereas the distance between Cu^{II} ions, which may potentially interact through stacking dpe fragments, is 14.2290(7) Å.

Compound 5. The crystal of **5** is built from binuclear TTF-containing cations $[Cu_2(LH)_2(TTF–CH=CH–py)(H_2O)]^{2+}$, anions ClO_4^- and isolated solvent molecules (which could not be localised because of disorder and were removed by SQUEEZE procedure implemented in PLATON[10]) (Fig. 7). Each Cu^{II} ion in **5** is located in a square-pyramidal donor set ($\tau = 0.10$ for Cu(1) and 0.01 for Cu(2)),[9] where positions in the base of the pyramids are occupied by four nitrogen atoms of two LH^- (oximato- and imino-groups). Axial positions of these square pyramids are filled with the N-atom of the pyridine ring of TTF–CH=CH–py (in the case of Cu(1)) or a coordinated water molecule (in the case of Cu(2)), and these axial ligands are located on the "external sides" of the V-shape molecule. As in the case of compounds **1–4**, Cu–N bonds with nitrogen atoms in the basement of square pyramid are shorter, than the bonds with donor atoms in axial positions (average bond length Cu–N_{basal} is 2.01 Å, while Cu(2)–O(5) is 2.278(3) Å and Cu(1)–N(9) is 2.203(3) Å, Table 5).

Similar to the above structures, in compound **5** there are donor atoms under the basement of both square pyramidal

Table 4 Selected bond lengths and distances for **4**

Bond	Length, Å	Bond	Length, Å
Cu(1)–N(1)	1.985(4)	Cu(1)–N(2)	2.052(3)
Cu(1)–N(3)	1.994(3)	Cu(1)–N(5)	2.223(4)
Cu(1)–N(4)	2.043(4)	O(1)–O(2)	2.438(5)

Table 5 Selected bond lengths and distances for **5**

Bond	Length, Å	Bond	Length, Å
Cu(1)–N(1)	1.997(3)	Cu(2)–N(5)	1.977(3)
Cu(1)–N(2)	2.051(3)	Cu(2)–N(6)	2.043(3)
Cu(1)–N(3)	1.986(3)	Cu(2)–N(7)	1.981(3)
Cu(1)–N(4)	2.044(3)	Cu(2)–N(8)	2.016(3)
Cu(1)–N(9)	2.203(3)	Cu(2)–O(5)	2.278(3)

chromophores of Cu^{II} ions, which fill the coordination environments of Cu^{II} to the highly distorted octahedra –O atom of perchlorate (Fig. 7) located at 3.088(5) Å from Cu(1), and the S(3)″ atom of TTF–CH=CH–py of the neighboring cation is located 3.473(2) Å from Cu(2). Intramolecular Cu–Cu separation in **5** is 7.1940(7) Å, and the intermolecular Cu–Cu distance through stacking TTF–CH=CH–py ligands is 18.2631(8) Å.

Coordinated TTF–CH=CH–py molecules are almost planar (the largest deviation from the mean plane is 0.217(6) Å (for C(40) atom of TTF), and they are located in parallel planes, similarly to dpe molecules in **4**. The separation between mean planes of neighbouring TTF–CH=CH–py molecules is 3.605(5) Å (almost the same as the distance between dpe planes in **4**, which is equal to 3.598(5) Å) (Fig. 8). A rather short separation between these planes may be caused by π-stacking interactions of TTF fragments of one molecule and pyridine rings of neighbouring molecule. In a contrast to TTF-containing compound **2**, "purely organic" and "metal-containing" components in **5** are covalently-bonded.

The C–C bond between two heterocyclic rings of TTF–CH=CH–py C(38)–C(39) is 1.355(6) Å, which is consistent with the neutral form of this molecule.[8]

The composition of compound **5** in respect to the Cu_2:pyridine ratio is the same, as in the case of **3** (one pyridine-containing molecule per one Cu_2 unit), but due to the stacking of organic ligands the crystal packing of **5** is more similar to the crystal packing of **4**, which has two pyridine-containing molecules per one Cu_2 unit. It seems that the presence of stacking is governed more by the nature of organic ligand rather than by the quantity of such ligands in the molecule. Addition of one π-bond to the molecule, containing aromatic systems (C=C bond in dpe) or replacement of pyridine ring by TTF–CH=CH– (TTF–CH=CH–py compared to bipy) favors the formation of π-stacks in the crystal.

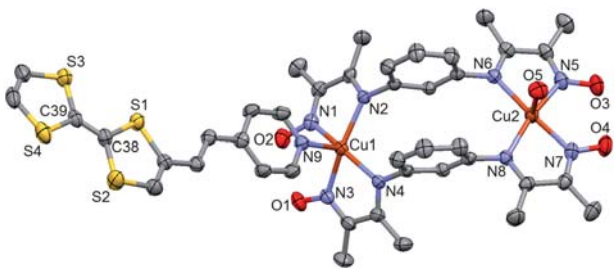

Fig. 7 ORTEP view of the complex $Cu_2(LH)_2(TTF–CH=CH–py)(H_2O)(ClO_4)_2$ (**5**). Thermal ellipsoids are drawn at 30% probability. Hydrogen atoms, perchlorate anion and molecules of crystallization are omitted for clarity.

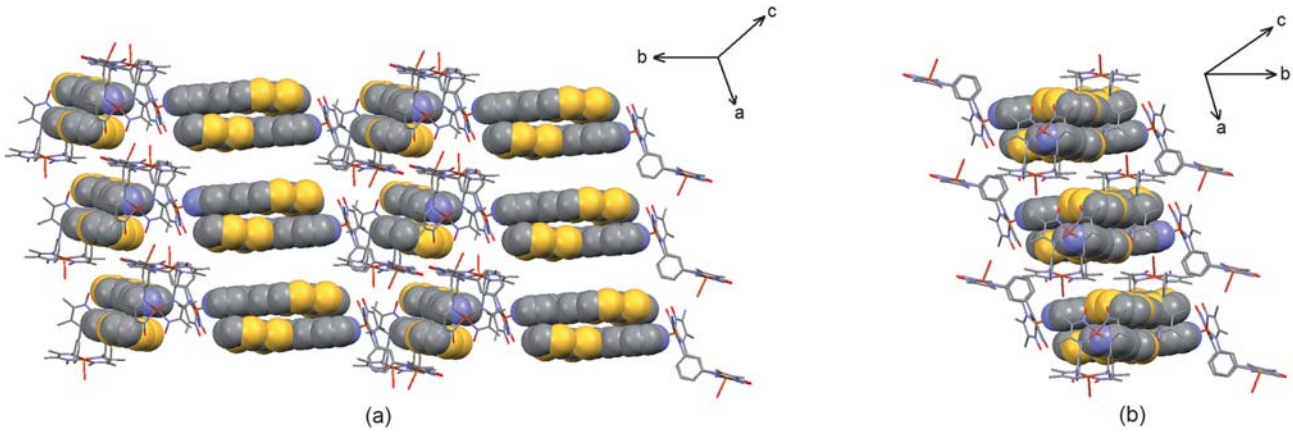

Fig. 8 Crystal packing of **5** highlighting the formation of dimers of TTF–CH = CH–Py in which the donors are "head-to-tail" stacked (space fill) (a). (b) Enclosing of the donors by the inorganic dinuclear Cu^{II} complexes (capped sticks).

Magnetic properties

Magnetic properties of the complexes **1–5** were characterized by the temperature dependence of the molar magnetic susceptibility, χ_M, in the range 2 to 300 K.

Compound 1. At 300 K $\chi_M T$ is equal to 0.85 cm^3 K mol^{-1}, which is consistent with the value expected for two non-interacting Cu^{II} ions with $g = 2.1$ (0.83 cm^3 K mol^{-1}). Compound **1** may be considered as an alternating chain, consisting of binuclear units (exchange of Cu^{II} paramagnetic centers through a 1,3-phenylene bridge), and each such unit is linked by a Cu–O bond (2.581(3) Å). As the approximation, magnetic properties were fit using slightly modified Bleaney–Bowers model with the Hamiltonian $H = -JS_1S_2$,[11] and interdimer coupling was taken into account by introduction of the term corresponding to the molecular field (zJ').[12] In order to avoid over parametrization we introduced temperature-independent paramagnetism (*tip*) in the model for compound **1** and other complexes as non-zero fitting parameter only in the cases where it improved the fit.

The best fit, presented in Fig. 9, corresponds to $J = +11.4(4)$ cm^{-1}, $g = 2.095(3)$, $zJ' = +0.735(9)$ cm^{-1} ($R^2 = 2.8 \times 10^{-4}$, here and in the whole text $R^2 = \Sigma(\chi_M T_{calc.} - \chi_M T_{obs.})^2/\Sigma(\chi_M T_{obs.})^2$).

The ESR spectrum of **1** contains a narrow signal at $g = 2.092$ (solid sample, 298 K), which perfectly agrees with the g-value, estimated from magnetochemical measurements.

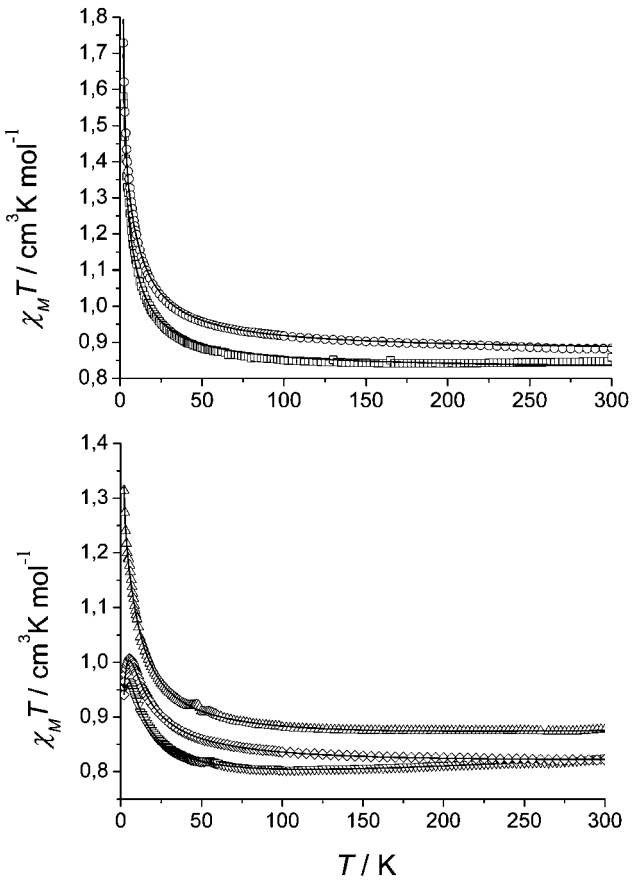

Fig. 9 $\chi_M T$ *vs.* T curves for 1 (□), 2 (○) (top), 3 (△), 4 (▽) and 5 (◇) (bottom). Solid lines correspond to the best fits with parameters from text.

Compound 2. The room-temperature value of $\chi_M T$ is equal to 0.89 cm^3 K mol^{-1} (the value, expected for two non-interacting Cu^{II} ions with $g = 2.15$ is 0.87 cm^3 K mol^{-1}). On cooling $\chi_M T$ monotonously increased to 1.73 cm^3 K mol^{-1} at 2 K. Data were fit using the same approach as for **1**; the best fit for **2** corresponded to $J = +13.4(2)$ cm^{-1}, $g = 2.159(2)$ and $zJ' = +0.731(7)$ cm^{-1} ($R^2 = 1.2 \times 10^{-4}$). The ESR signal of compound **2** is more broad compared to the ESR of **1** (solid sample, 298 K). The principal component of this spectrum has $g = 2.093$, and there is overlap with one more signal with g about 2.16, which may be assigned to $g_\perp$ and $g_\parallel$, respectively. In this case $g_{average}$ is 2.12, which is quite consistent with g, derived from $\chi_M T$ *vs.* T curve fitting.

Compound 3. At 300 K, $\chi_M T$ for **3** is equal to 0.88 cm^3 K mol^{-1}, which is consistent with the value expected for two non-interacting Cu^{II} ions with $g = 2.1$ (0.83 cm^3 K mol^{-1}). Since exchange interactions through bipy bridge were expected to be negligibly small,[13] a slightly modified Bleaney–Bowers model taking into account molecular field and *tip* was used to reproduce magnetic data. The best fit, presented in Fig. 9, corresponds to $J = +10.6(1)$ cm^{-1}, $g = 2.122(1)$, $zJ' = +0.308(4)$ cm^{-1} and $tip = 7.0(5) \cdot 10^{-5}$ ($R^2 = 9.2 \times 10^{-6}$).

Compound 4. The form of $\chi_M T$ *vs.* T curve for **4** is different from curves of compounds **1–3**. At 300 K $\chi_M T$ for **4** is 0.82 cm^3 K mol^{-1}. When lowering T, $\chi_M T$ decreases, reaching a minimum at 100 K (0.80 cm^3 K mol^{-1}), after which it grows to 0.96 cm^3 K mol^{-1} at 4.5 K before falling down to 0.95 cm^3 K mol^{-1} at 2 K. Though the dominating interactions in **4** are ferromagnetic, and these interactions correspond to exchange coupling through the 1,3-phenylene bridge in binuclear unit, it may be supposed from the shape of the $\chi_M T$ *vs.* T curve that the coupling between binuclear cations is antiferromagnetic. Such antiferromagnetism may originate from the exchange through coplanar coordinated dpe molecules, located at 3.598(5) Å (separation between mean planes of dpe molecules) from each other at 300 K.

Magnetic data were fit using the same model as for **1**, the best fit, presented on Fig. 9, corresponds to $J = +9.92(8)$ cm^{-1}, $g = 2.015(1)$, $zJ' = -0.158(3)$ and $tip = 1.80(2)\cdot10^{-4}$ ($R^2 = 4.0 \times 10^{-6}$). Remarkably, the calculated curve fits the experimental data in the whole temperature range, including a broad minimum at 100 K and a sharp maximum at 4.5 K. The room-temperature value of $\chi_M T$ for **4** (0.82 cm^3 K mol^{-1}) is higher than expected value for two non-interacting Cu^{II} ions with $g = 2.0$ (0.75 cm^3 K mol^{-1}), but it may be explained by a rather high contribution of temperature-independent paramagnetism.

Compound 5. At 300 K, $\chi_M T$ for **5** was equal to 0.82 cm^3 K mol^{-1} (Fig. 9), which is consistent with the value, expected for two non-interacting Cu^{II} ions with $g = 2.1$ (0.83 cm^3 K mol^{-1}). On cooling $\chi_M T$ increases to 1.01 cm^3 K mol^{-1} at 5.5 K and then decreases to 0.94 cm^3 K mol^{-1} at 2 K.

The best fit for **5**, performed as described above for **1**, corresponded to the $J = +10.90(7)$ cm^{-1}, $g = 2.072(1)$, $zJ' = -0.290(2)$ cm^{-1} and $tip = 2.0(2)\cdot10^{-5}$ ($R^2 = 1.6 \times 10^{-6}$). The ESR spectrum of compound **5** (solid sample, 298 K) is similar to the spectrum of **1**. The spectrum contains a narrow signal at $g = 2.098$. This value is consistent with g, calculated from magnetochemical data. Coordination of TTF–CH=CH–py to $Cu_2(LH)_2^{2+}$ almost did not change the g-factor of Cu^{II} ions. g-factors of "starting compounds" **1** and **5** are more similar, that g-factors of **1** and **2**, though TTF-carboxylate is not covalenly bonded to Cu^{II} in **2**, and TTF–CH=CH–py is bonded to Cu^{II} in **5**. The difference between g-factors of **2** and **1** or **5** is probably caused by the coordination of methanol in **2**.

Though the closest Cu–Cu separations in compounds **1–3** are not intradimer separations, but the distances between Cu^{II} ions through Cu–O contacts, dominating exchange interactions are transferred through the phenylene bridge, as it may be concluded from the similarity of J values for complexes **1–3**, which have intermolecular Cu–O contacts, and **4–5**, which do not have such contacts. This observation may be explained by the location of the unpaired electrons of Cu^{II} ions on d orbitals, lying in N_4 planes, and almost zero density of unpaired spin on the d orbital, which is involved in intermolecular interactions (through axial Cu–O contacts or bonds). In all compounds, considered in this study, dominating ferromagnetic exchange interactions are caused by coupling of 1/2 spins of Cu^{II} ions through a 1,3-phenylene bridge, which is consistent with magnetic properties of reported complexes possessing similar bridging units.[4] The J values for **1–5** range from +9.92(8) cm^{-1} to +13.4(2) cm^{-1}. For comparison, in the case of dinuclear Cu^{II} complexes with N,N-1,3-phenylenebis(oxamate) (L′), $Na_4Cu_2L'_2$, and 2,4,6-trimethyl-1,3-phenylenebis(oxamate) (L′), $Na_4Cu_2L'_2$, containing 1,3-phenylene bridges similar to the one in $Cu_2(LH)_2$, J values were found to be +16.8 and +11 cm^{-1} (here and below for the Hamiltonian $H = -JS_1S_2$).[4a,4h] For $Cu_2(L''')_2$ (where $H_2L''' = 1:2$ Schiff base from 1,3-diaminobenzene and 2,4-pentanedione) J was found to be +14.56 cm^{-1}.[4b] Close values of J, found in **1–5** and in reported Cu^{II} complexes with a 1,3-phenylene bridge, may be the additional evidence for the assignment of J in **1–5** to intramolecular coupling through LH^-. In addition it may be noted, that intermolecular Cu–O contacts in **1–5** have some similarity with out-of-plane oximato bridges in $Cu(N–O)_2Cu$ metallocycles.[14] It was shown that the values of J for Cu–Cu exchange interactions in such cycles correlate with the angle N–O–Cu, denoted as α, and become negative at $\alpha > 107°$.[14b] The angles N–O–Cu in compounds **1–3** lie in the range between 136 and 157°, and according to the above correlation exchange interactions through this pathway should be antiferromagnetic. Thus, positive values of J, found for **1–3**, can be attributed to exchange through a 1,3-phenylene bridge.

Non-zero values of zJ' may be evidence of some intermolecular interactions. For complexes **1–3**, where no π-stacking was observed in the crystal, zJ' are positive, whereas for compounds **4** and **5**, where π-stacking of dpe or TTF–CH=CH–py units was found, respectively, zJ' values are negative.

It was possible to fit $\chi_M T$ *vs.* T curves for compound **1** and **2** without contribution of *tip*, and for compounds **3–5** obtained values of *tip* are consistent with the one, typical for Cu^{II} dimers (1.2×10^{-4}).[12]

Redox behaviour

Redox properties were studied for compound **5**, containing TTF ligand, covalently-bonded to Cu^{II}, and for compound **1** for comparison. The measurements were performed in solutions in non-coordinating solvent (dichloromethane) in order to minimise dissociation of the compound **5**.

Pure TTF–CH=CH–py undergoes two redox processes in solution in CH_2Cl_2 at $E_{1/2}(1) = 0.423$ V and $E_{1/2}(2) = 0.855$ V *vs.* SCE. The values of redox-potentials are very similar to reported redox-potentials of this compound in acetonitrile (0.441 V and 0.804 V in acetonitrile *vs.* SCE[8a]). The first wave $E(1)$ is associated with one-electron reversible process TTF–CH=CH–py/TTF–CH = CH–py$^{\bullet+}$, whereas the second $E(2)$ corresponds to one-electron reversible process TTF–CH=CH–py$^{\bullet+}$/TTF–CH=CH–py^{2+}.[8a,15]

Redox behavior of binuclear complex **1** in CH_2Cl_2 is more complicated. At the first scan there is only one wave at $E_c = 0.130$ V, which may correspond to irreversible reduction $Cu^{2+} \rightarrow Cu^{+}$, as it was found in similar systems.[7b,c,16] At the second scan the potential $E_c(1)$ shifts toward a cathodic region (to 0.082 V), and counter-peaks appear at $E_a(1) = 0.486$ V and $E_a(2) = 0.886$ V. Further scans result in increase of both E_a (to 0.56 V and 1.06 V, respectively, after 7 scans) and decrease of E_c (to 0.00 V after 7 scans), along with a gradual increase of the currents of all processes. Such behaviour may be explained by adsorption of the reaction products on the surface of the electrode followed by its oxidation (such as $Cu^{2+} \rightarrow Cu^{3+}$) at potentials above 0.4 V.

The CV curve of compound **5** at the first scan shows two redox processes. The first process is characterized by a reduction peak

at $E_c(1) = 0.282$ V, which shifts to 0.238 V at the second scan, and is stabilized at 0.200 V after the third scan. A corresponding oxidation process is observed at $E_a(1) = 0.474$ V and is insensitive to the number of scans. These two waves can be assigned to semi-reversible reduction and oxidation of the same redox-center, with $E_{1/2}(1) = 0.378$ V and $\Delta E = 0.192$ V. The second process was observed at $E_{1/2}(2) = 0.838$ V ($\Delta E = 0.110$ V) and its potential did not change at repeated scans.

The redox-processes in fresh solution of **5** (first scan) may be assigned to coordinated TTF–CH=CH–py. There is no significant shift of the values of both potentials $E(1)$ and $E(2)$ in **5** compared to those observed with free TTF–CH=CH–py, which may be concluded taking into account poor reversibility of the process, corresponding to the $E(1)$ potential in **5**. This fact may be explained by the coordination of the N atom of this ligand to an axial position in the coordination sphere of Cu^{II} in **5**. In this compound the Cu–N_{py} bond corresponds to the Jahn–Teller axis of Cu^{II} chromophore, and hence the influence of metal ions on the distribution of electronic density within TTF–CH=CH–py is not significant.

When the experiment time increases, the electrochemical behavior of the solution of **5** resembles the superposition of CVA of TTF–CH=CH–py and CVA of compound **1**, which may be evidence of dissociation of **5** into $Cu_2(LH)_2^{2+}$ and TTF–CH=CH–py.

Regretfully, all attempts to isolate the compound containing oxidized TTF–CH=CH–py in order to measure its conducting properties were not successful.

Conclusions

It was shown that the use of polynuclear complexes with ferromagnetic exchange interactions as "building blocks" allowed the preparation of TTF-containing compounds with ferromagnetic exchange within the polymetallic core. Exchange interactions in dinuclear cation $Cu_2(LH)_2^{2+}$, used as a "building block", almost do not depend on the nature of ligands, coordinated to Cu^{II}, as it can be concluded from a comparison of the properties of several compounds containing this cation. For compounds **1–5** values of J lie between +9.92(8) cm^{-1} and +13.4(2) cm^{-1}, and for compounds, containing stacks of aromatic molecules in crystal structures (**4** and **5**) antiferromagnetic intermolecular interactions were found ($zJ' = -0.158(3)$ and $-0.290(2)$ cm^{-1}, respectively). The TTF–CH=CH–py ligand in $Cu_2(LH)_2$(TTF–CH=CH–py)$(H_2O)^{2+}$ may be electrochemically oxidized to a cation-radical form in the solution. The proposed strategy—assembling of ferromagnetically-coupled "building blocks" with TTF-containing ligands—may be used for the preparation of ferromagnetic conducting materials.

Experimental

Materials and measurements

Commercially available reagents (Aldrich, Merck) were used as received. Solvents were dried and distilled by standard procedures. TTF–CH=CH–py and TTF–CO_2 were prepared according to the literature procedures.[8a,17] ESR spectra were measured using BRUKER EMX X-band ESR spectrometer at the temperature 298 K. Magnetic measurements were performed using a Quantum Design MPMS SQUID magnetometer operating in the temperature range 2–300 K with a DC magnetic field up to 5 T on powdered samples. Raw data have been corrected for the contribution of the holder. Samples were measured in Teflon capsules, diamagnetic corrections were calculated using Pascal's constants.[12]

Table 6 Selected crystallographic data for **1–5**

	Compound **1**	Compound **2**	Compound **3**	Compound **4**	Compound **5**
Empirical formula	$C_{28}H_{33}Cl_2Cu_2N_8O_{14}$	$C_{37}H_{44}ClCu_2N_8O_{13}S_4$	$C_{38}H_{42}Cl_2Cu_2N_{10}O_{15}$	$C_{54}H_{60}Cl_2Cu_2N_{12}O_{14}$	$C_{41}H_{41}Cl_2Cu_2N_9O_{13}S_4$
Formula weight/g mol^{-1}	903.60	1099.57	1076.80	1299.14	1194.05
T/K	293(2)	293(2)	293(2)	293(2)	293(2)
Wavelength/Å	0.71073	0.71073	0.71073	0.71703	0.71703
Crystal system	Monoclinic	Monoclinic	Monoclinic	Monoclinic	Monoclinic
Space group	P21/c	P21/c	P21/a	*C*2/*c*	P21/n
a/Å	18.6057(3)	11.4326(3)	15.0633(3)	20.3545(4)	11.316(1)
b/Å	11.2046(2)	17.9255(7)	14.5216(3)	9.9403(2)	22.212(1)
c/[Å	18.7297(5)	23.2958(10)	21.9097(5)	30.9701(9)	23.497(1)
β (°)	103.224(1)	98.79(2)	95.005(8)	105.089(1)	97.312(1)
Volume/$Å^3$	3801.03(14)	4718.1(3)	4774.3(2)	6050.1(2)	5858.0(6)
Z	4	4	4	4	4
Calculated density/g cm^{-3}	1.579	1.548	1.498	1.428	1.354
Absorption coefficient/mm^{-1}	1.333	1.204	1.078	0.864	1.020
F(000)	1844	2260	2208	2696	2440
Theta range for data collection/°	0.99 to 27.49	0.988 to 27.52	1.00 to 28.28	1.00 to 30.03	0.997 to 27.48
Reflections collected	15089	20453	21102	14477	24794
Reflections unique	8651	10736	11784	8579	13389
R(int)	0.0374	0.0759	0.0414	0.0539	0.0338
Parameters	518	594	603	378	640
Goodness-of-fit on F^2	1.038	1.032	1.028	0.975	0.986
$R_1{}^a$ [$I > 2\sigma(I)$]	0.0670	0.1005	0.0770	0.0717	0.0609
w$R_2{}^b$ [$I > 2\sigma(I)$]	0.1771	0.2836	0.2247	0.1938	0.1792

^{a} $R_1 = \Sigma||F_o| - |F_c||/\Sigma\,|F_o|$. ^{b} $wR_2 = \{\Sigma[w\,(F_o^2 - F_c^2)^2]/\Sigma[w\,(F_o^2)^2]\}^{1/2}$.

Crystallographic data collection and structure determination

Single crystals of the title compounds were mounted on a Nonius four circle diffractometer equipped with a CCD camera and a graphite monochromated Mo Kα radiation source ($\lambda = 0.71073$ Å), from the Centre de Diffractométrie (CDFIX), Université de Rennes 1, France. Effective absorption correction was performed (SCALEPACK[18]). Structures of complexes were solved with a direct method using SHELXS–97[19] or Sir-97[20] and refined with full matrix least squares method on F^2 using the SHELXL–97[19] program. Crystallographic data are summarized in Table 6. CCDC deposition numbers for the compounds 1–5 are 756226–756230 respectively.

Caution. Though we did not have any problems working with perchlorates, such compounds are potentially explosive and should be handled with due caution.

Synthesis of $[Cu_2(LH)_2(H_2O)_2](ClO_4)_2$ (1)

1,3-Diaminobenzene (0.1 g, 9.26×10^{-4} mole) was dissolved in methanol (4 mL). To this solution a solution of butanedione monoxime 0.187 g (1.85×10^{-3} mole) in methanol (2 mL) was added and the reaction mixture was heated at 50 °C during 20 min. After this $Cu(ClO_4)_2 \cdot 6H_2O$ (0.343 g, 9.26×10^{-4} mole) in methanol (2 mL) was added to reaction mixture. Black amorphous precipitate quickly formed, the mixture was left for 2 days and during this time the amorphous solid transformed into microcrystals, which were filtered, washed with methanol (3 mL) and dried on air. Yield 0.250 g (60%). Anal. calcd. for $C_{28}H_{38}N_8O_{14}Cl_2Cu_2$ (908.67): C 37.0, H 4.22, N 12.3; found: C 37.1, H 4.20, N 12.3.

$Cu_2(LH)_2(CH_3OH)_2(TTF–CO_2)(ClO_4) \cdot H_2O$ (2)

0.100 g of $Cu_2L_2(H_2O)(ClO_4)_2$ (1.107×10^{-4} mole) was dissolved in 2 mL of acetonitrile and a solution of 1.107×10^{-4} mole of $TTF–CO_2^-Na^+$ (prepared *in situ* by reaction of 0.027 g of $TTF–CO_2H$ (1.107×10^{-4} mole) with equimolar quantity of NaOH in methanol) in 10 mL of methanol was added. Reaction mixture was quickly filtered and left undisturbed for 1 day. Dark greenish-brown crystals were collected, washed with methanol (5 mL) and air dried. Yield 0.095 g (80%). Anal. calcd. for $C_{37}H_{47}N_8O_{13}ClS_4Cu_2$ (1102.65): C 40.3, H 4.30, N 10.2, found: C 39.8, H 3.92, N 10.0.

Synthesis of $\{[Cu_2(LH)_2(bipy)](ClO_4)_2\}_n \cdot 2nH_2O$ (3)

Compound **1** (0.050 g, 5.5×10^{-5} mole) was dissolved in methanol (5 mL) at 50 °C, the solution was cooled to room temperature, filtered and diluted with 2-propanol (2 mL). Solid 4,4-bipyridine (0.017 g, 1.1×10^{-4} mole, 2^x excess) was dissolved in the solution, after which the mixture was left for 2 days. The crystalline product was filtered, washed with the mixture of methanol and 2-propanol (3 mL, 1 : 1 by volume) and dried in air. Yield 0.047 g (80%). Anal. calcd. for $C_{38}H_{46}N_{10}O_{14}Cl_2Cu_2$ (1064.85): C 42.9, H 4.35, N 13.2; found: C 42.8, H 4.41, N 13.0.

Synthesis of $[Cu_2(LH)_2(dpe)_2](ClO_4)_2 \cdot 2CH_3OH$ (4)

Compound **1** (0.050 g, 5.5×10^{-5} mole) was dissolved in methanol (5 mL) at 50 °C, solution was cooled to room temperature, filtered and diluted with 2-propanol (2 mL). Solid *trans*-1,2-dipyridylethylene (0.020 g, 1.1×10^{-4} mole) was dissolved in the solution, after which the mixture was left for 2 days. Crystalline product was filtered, washed with the mixture of methanol and 2-propanol (3 mL, 1 : 1 by volume) and dried in air. Yield 0.060 g (83%). Anal. calcd. for $C_{54}H_{62}N_{12}O_{14}Cl_2Cu_2$ (1301.17): C 49.8, H 4.80, N 12.9; found: C 49.9, H 4.60, N 12.8.

$Cu_2(LH)_2(TTF–CH{=}CH–py)(H_2O)(ClO_4)_2 \cdot 1.5H_2O$ (5)

0.100 g of $Cu_2L_2(H_2O)(ClO_4)_2$ (1.107×10^{-4} mole) was dissolved in 8 mL of nitromethane, and 0.034 g of TTF–CH=CH–py (1.107×10^{-4} mole) were added. Reaction mixture was stirred until complete dissolution of TTF–CH=CH–py, filtered from some remaining impurities and placed in a dessicator with ether. Diffusion of ether afforded black-brown crystals in 2 weeks, which were collected by filtration, washed with ether and recrystallized in the same manner. Yield 0.065 g (50%). Anal. calcd. for $C_{41}H_{48}N_9O_{14,5}Cl_2S_4Cu_2$ (1225.16): C 40.2, H 3.95, N 10.3; found C 40.5, H 3.95, N 10.0.

Acknowledgements

This work was partially supported by exchange program of CNRS-NAS of Ukraine. S.V.K. thanks Région Bretagne for post-doc support. This work also was supported in part by the EU through MAGMANet.

References

1 (*a*) A. Kobayashi, E. Fujiwara and H. Kobayashi, *Chem. Rev.*, 2004, **104**, 5243–5264; (*b*) T. Enoki and A. Miyazaki, *Chem. Rev.*, 2004, **104**, 5449–5477; (*c*) E. Coronado and P. Day, *Chem. Rev.*, 2004, **104**, 5419–5448; (*d*) L. Ouahab and T. Enoki, *Eur. J. Inorg. Chem.*, 2004, 933–941; (*e*) H. Fujiwara, K. Wada, T. Hiraoka, T. Hayashi, T. Sugimoto, H. Nakazumi, K. Yokogawa, M. Teramura, S. Yasuzuka, K. Murata and T. Mori, *J. Am. Chem. Soc.*, 2005, **127**, 14166–14167; (*f*) R. Kato, *Bull. Chem. Soc. Jpn.*, 2000, **73**, 515–534; (*g*) D. Maspoch, D. Ruiz-Molina and J. Veciana, *Chem. Soc. Rev.*, 2007, **36**, 770–818; (*h*) B. V. Harbuzaru, A. Corma, F. Rey, P. Atienzar, J. L. Jordá, H. García, D. Ananias, L. D. Carlos and J. Rocha, *Angew. Chem., Int. Ed.*, 2008, **47**, 1080–1083.

2 (*a*) H. Hiraga, H. Miyasaka, R. Clérac, M. Fourmigué and M. Yamashita, *Inorg. Chem.*, 2009, **48**, 2887–2898; (*b*) H. Hiraga, H. Miyasaka, K. Nakata, T. Kajiwara, S. Takaishi, Y. Oshima, H. Nojiri and M. Yamashita, *Inorg. Chem.*, 2007, **46**, 9661–9671.

3 (*a*) D. Lorcy, N. Bellec, M. Fourmigue and N. Avarvari, *Coord. Chem. Rev.*, 2009, **253**, 1398–1438; (*b*) K. S. Gavrilenko, Y. Le Gal, O. Cador, S. Golhen and L. Ouahab, *Chem. Commun.*, 2007, 280–282; (*c*) N. Benbellat, K. S. Gavrilenko, Y. Le Gal, O. Cador, S. Golhen, A. Gouasmia, J.-M. Fabre and L. Ouahab, *Inorg. Chem.*, 2006, **45**, 10440–10442; (*d*) L. Ouahab, F. Iwahori, S. Golhen, R. Carlier and J. P. Sutter, *Synth. Met.*, 2003, **133–134**, 505–507; (*e*) G. Cosquer, F. Pointillart, Y. Le Gal, S. Golhen, O. Cador and L. Ouahab, *Dalton Trans.*, 2009, 3495–3502; (*f*) F. Pointillart, O. Maury, Y. Le Gal, S. Golhen, O. Cador and L. Ouahab, *Inorg. Chem.*, 2009, **48**, 7421–7429; (*g*) F. Pointillart, Y. Le Gal, S. Golhen, O. Cador and L. Ouahab, *Inorg. Chem.*, 2009, **48**, 4631–4633.

4 (*a*) I. Fernández, R. Ruiz, J. Faus, M. Julve, F. Lloret, J. Cano, X. Ottenwaelder, Y. Journaux and M. C. Muñoz, *Angew. Chem., Int. Ed.*, 2001, **40**, 3039–3042; (*b*) A. R. Paital, T. Mitra, D. Ray, W. T. Wong, J. Ribas-Ariño, J. J. Novoa, J. Ribas and G. Aromí, *Chem. Commun.*, 2005, 5172–5174; (*c*) T. Glaser, M. Gerenkamp and R. Fröhlich, *Angew. Chem., Int. Ed.*, 2002, **41**, 3823–3825; (*d*) E. Pardo, K. Bernot, M. Julve, F. Lloret, J. Cano, R. Ruiz-García, F. S. Delgado, C. Ruiz-Pérez, X. Ottenwaelder and Y. Journaux,

Inorg. Chem., 2004, **43**, 2768–2770; (*e*) X. Ottenwaelder, J. Cano, Y. Journaux, E. Rivière, C. Brennan, M. Nierlich and R. Ruiz-García, *Angew. Chem., Int. Ed.*, 2004, **43**, 850–852; (*f*) C. L. M. Pereira, E. F. Pedroso, H. O. Stumpf, M. A. Novak, L. Ricard, R. Ruiz-García, E. Rivière and Y. Journaux, *Angew. Chem., Int. Ed.*, 2004, **43**, 956–958; (*g*) E. Pardo, R. Ruiz-García, J. Cano, X. Ottenwaelder, R. Lescouëzec, Y. Journaux, F. Lloret and M. Julve, *Dalton Trans.*, 2008, 2780–2805; (*h*) E. Pardo, R. Ruiz-García, F. Lloret, M. Julve, J. Cano, J. Pasán, C. Ruiz-Pérez, Y. Filali, L.-M. Chamoreau and Y. Journaux, *Inorg. Chem.*, 2007, **46**, 4504–4514.

5 (*a*) S. V. Kolotilov, O. Cador, K. S. Gavrilenko, S. Golhen, L. Ouahab and V. V. Pavlishchuk, *Eur. J. Inorg. Chem.*, 2010, 1255–1266; (*b*) E. A. Mikhalyova, S. V. Kolotilov, K. S. Gavrilenko, P. G. Nagornyi, S. Golhen, L. Ouahab and V. V. Pavlishchuk, *Theor. Exp. Chem.*, 2008, **44**, 245–251.

6 A. S. El-Tabl, *Transition Met. Chem.*, 1997, **22**, 400–405.

7 (*a*) S. V. Kolotilov, D. Schollmeyer, L. K. Thompson, V. Golub, A. W. Addison and V. V. Pavlishchuk, *Dalton Trans.*, 2008, 3007–3014; (*b*) M. J. Prushan, A. W. Addison and R. J. Butcher, *Inorg. Chim. Acta*, 2000, **300–302**, 992–1003; (*c*) V. V. Pavlishchuk, A. W. Addison, R. J. Butcher and R. P. F. Kanters, *Inorg. Chem.*, 1994, **33**, 397–399.

8 (*a*) R. Andreu, I. Malfant, P. G. Lacroix and P. Cassoux, *Eur. J. Org. Chem.*, 2000, 737–741; (*b*) F. Iwahori, S. Golhen, L. Ouahab, R. Carlier and J.-P. Sutter, *Inorg. Chem.*, 2001, **40**, 6541–6542; (*c*) C. Katayama, M. Honda, H. Kumagai, J. Tanaka, G. Saito and H. Inokuchi, *Bull. Chem. Soc. Jpn.*, 1985, **58**, 2272–2278.

9 A. Addison, T. N. Rao, J. Reedijk, J. Rijn and G. Verschoor, *J. Chem. Soc., Dalton Trans.*, 1984, 1349–1356.

10 P. v. d. Sluis and A. L. Spek, *Acta Crystallogr., Sect. A: Found. Crystallogr.*, 1990, **46**, 194–201.

11 E. Sinn, *Coord. Chem. Rev.*, 1970, **5**, 313–347.

12 O. Kahn, *Molecular Magnetism*, Wiley-VCH, Weinheim, Germany, 1993.

13 (*a*) H. W. Park, S. M. Sung, K. S. Min, H. Bang and M. P. Suh, *Eur. J. Inorg. Chem.*, 2001, 2857–2863; (*b*) M. Julve, M. Verdaguer, J. Faus, F. Tinti, J. Moratal, A. Monge and E. Gutierrez-Puebla, *Inorg. Chem.*, 1987, **26**, 3520–3527; (*c*) M. S. Haddad, D. N. Hendrickson, J. P. Cannady, R. S. Drago and D. S. Bieksza, *J. Am. Chem. Soc.*, 1979, **101**, 898–906; (*d*) S. V. Kolotilov, O. Cador, S. Golhen, O. Shvets, V. G. Ilyin, V. V. Pavlishchuk and L. Ouahab, *Inorg. Chim. Acta*, 2007, **360**, 1883–1889.

14 (*a*) P. Chaudhuri, *Coord. Chem. Rev.*, 2003, **243**, 143–190; (*b*) B. Cervera, R. Ruiz, F. Lloret, M. Julve, J. Cano, J. Faus, C. Bois and J. Mrozinski, *J. Chem. Soc., Dalton Trans.*, 1997, 395–401.

15 K. B. Simonsen, K. Zong, R. D. Rogers and M. P. Cava, *J. Org. Chem.*, 1997, **62**, 679–686.

16 M. Kato, T. Tanase and M. Mikuriya, *Inorg. Chem.*, 2006, **45**, 2925–2941.

17 D. C. Green, *J. Org. Chem.*, 1979, **44**, 1476–1479.

18 Z. Otwinowski and W. Minor, *"Processing of X-ray Diffraction Data Collected in Oscillation Mode", Methods in Enzymology, Volume 276: Macromolecular Crystallography, part A*, pp. 307–326, 1997, ed. C. W. Carter, Jr. & R. M. Sweet, Academic Press.

19 (*a*) G. M. Sheldrick, *SHELXL-97, Program for refinement of crystal structures*, University of Göttingen, Germany, 1997, release 97-2; (*b*) G. M. Sheldrick, *SHELXL-93, Program for refinement of crystal structures*, University of Göttingen, Germany, 1993.

20 A. Altomare, M. C. Burla, M. Camalli, G. L. Cascarano, C. Giacovazzo, A. Guagliardi, A. G. G. Moliterni, G. Polidori and R. Spagna, *J. Appl. Crystallogr.*, 1999, **32**, 115–119.

